INDUCTION HEATING ANALYSIS VALIDATION OF CF/PEKK LAMINATES WITH MAGNETIC FLUX CONTROLLER

Waruna Seneviratne*, John Tomblin, Jerome J.C. Teoh, Brandon L. Saathoff, and Nicholas A. Smith
National Institute for Aviation Research (NIAR), Wichita State University (WSU)
1845 Fairmount St.
Wichita, KS 67206

ABSTRACT

High-strength fiber-reinforced thermoplastic composites are beginning to replace their traditional thermoset counterparts in the aerospace industry. Due to the electrically conductive nature of carbon fiber, induction welding can be leveraged to achieve valuable weight savings in certain subassemblies and structural joints by elimination of fasteners. In order to reduce trial and error while developing the induction welding process, a numerical model was employed to investigate the inductive heating on thermoplastic composite material. In this work, a CF/PEKK laminate and induction coils with and without a flux concentrator was considered. The simulated temperature data is then validated against experimental data that included cross-ply and quasi-isotropic stacking sequences. Critical factors that affect the heating rate and distribution were shown to be the laminate stacking sequence and the addition of the magnetic flux controller on the induction coil.
Keywords: thermoplastic composites, induction welding, magnetic flux controller
Corresponding author:

1. INTRODUCTION

Given the increased demand for high rate production of aircraft structures, a significant emphasis has been put on the implementation of reinforced thermoplastic composite materials. Thermoplastic composites have previously shown potential for reducing manufacturing cycle time and cost over traditional reinforced thermoset composites. In many past uses, thermoplastic composites were processed using similar procedures as thermoset composites (hand layup and autoclave processing). This was proven to be very costly at scale due to the tooling and bagging requirements for the high processing temperatures associated with thermoplastics. Recent advances in the thermoplastic material quality and improved automated processing equipment such as automated fiber placement (AFP) machines with advanced heating such as laser has provided a new solution for economically implementing reinforced thermoplastic composites in a high-rate production environment. With this, developing reliable joining strategies that can be efficiently employed into commercial production is necessary. Unlike thermosetting polymers, thermoplastic polymers offer the ability to be heated and formed repeatedly without any degradation to the polymer. Due to this capability, non-traditional joining approaches such as induction welding can be applied to offer significant weight and cost savings over adhesive bonding and mechanical fastening joining techniques [1].

In the induction welding operation, alternating current is passed through an induction coil to produce a high frequency electromagnetic field. This induces electric current known as eddy currents into the nearby materials (carbon fibers or susceptor) to generate resistive heat and subsequently melt the polymer in each substrate. Under pressure, intimate contact is formed at the interface between the two substrates, and the materials flow into one another. As the material is cooled, the polymer solidifies and the substrates are consolidated. The induction weld quality and performance is largely governed by the temperature and pressure parameters applied in the welding process. Generating heat efficiently and uniformly at the interface of the joint requires an optimized induction coil design for each use case. Designing induction coils to have a uniform temperature distribution at the joint interface is challenging and many variables must be considered (i.e., edge effects, magnetic flux controllers, variable material properties, and boundary conditions) [2]. Depending on the joint geometry (see examples shown in Figure 1), the optimum coil geometry and heating strategy will change. This can result in a significant amount of trial-and-error experimental studies to optimize the induction welding process. Therefore, induction welding simulations are employed to help optimize the processing parameters associated with induction welding and to reduce the dependency on experiments during design optimization cycle.

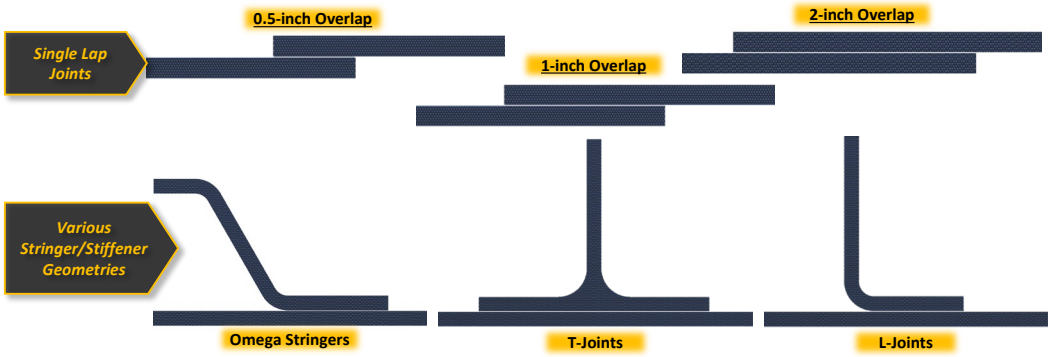

Figure 1. Various joint geometries.

In this study, cross-ply (CP) and quasi-isotropic (QI) CF/PEKK laminates were heated using various induction coil designs to validate analysis predictions. A magnetic flux controller (MFC) was used to help concentrate the magnetic field density to the laminate. This was numerically modeled and the temperature-time heating behavior was benchmarked. Overall, the influence of stacking sequence on the induction heating response was evaluated for multiple induction coil geometries. Numerical models developed in this research can then be used for designing the induction welding process for various joint geometries.

1.1 Overview of Induction Physics

In the induction welding process, there are a few physical phenomena that need to be considered. As electric current passes through a coil, a magnetic field is generated. When a conductive material is placed inside this magnetic field, eddy currents are induced in that material. Classical electromagnetism, which is described by Maxwell's equations, is used to model this effect. Although some other methods of heat generation have been considered in other work [3–5], many researchers [6–8] have found the primary method of heat generation in thermoplastic composites to be Joule heating. This work considers only the Joule heating mechanism, which occurs when electric current passes through a conductive material with some resistivity. In differential form, the relevant equations to describe the electromagnetic and heating physics are:

- Gauss's law, which relates the electric field, E, with the electric charge density ρ and the electric constant, ϵ_0.

$$\nabla \cdot E = \frac{\rho}{\epsilon_0} \quad [1]$$

- Gauss's law for magnetism, which states that the divergence of the magnetic field, B, is zero.

$$\nabla \cdot B = 0 \quad [2]$$

- Faraday's law of induction, which relates the time-varying magnetic field (B) with the spatial electric field (E).

$$\nabla \times \mathrm{E} = -\frac{\partial B}{\partial t} \quad [3]$$

- Ampère's circuital law with Maxwell's correction, which relates the magnetic field around a closed loop with the electric field,

$$\nabla \times \mathrm{B} = \mu_0 J + \mu_0 \epsilon_0 \frac{\partial E}{\partial t} \quad [4]$$

where μ_0 is the magnetic permittivity and J is the electric current density, which is related to the electric field, E, by the material's conductivity, σ, using Ohm's Law

$$\mathrm{J} = \sigma \cdot \mathrm{E} \quad [5]$$

- Joule heating describes the heat generated, Q, in a resistive material,

$$\mathrm{Q} = \mathrm{J} \cdot \mathrm{E} \quad [6]$$

and the heat transfer in the system is modeled using the heat equation,

$$\mathrm{Q} = \rho \mathrm{c_p} \frac{\partial T}{\partial t} - \nabla \cdot (\lambda \nabla T) \quad [7]$$

where ρ is density, $\mathrm{c_p}$ is specific heat capacity, T is temperature and λ is thermal conductivity.

2. EXPERIMENTAL SETUP

Experimental heating studies were performed on Solvay APC CP and QI laminates with layups of $[0/90]_{4S}$ and $[45/0/\text{-}45/90]_{2S}$, respectively. Two different induction coil designs including a single hairpin coil and a 3-turn helical coil were used at a fixed offset distance of 12.4 mm (Figure 2). Heat output was monitored on the backside of the laminate using a Gobi 640 Long Wave Infrared (LWIR) camera as shown in Figure 2.

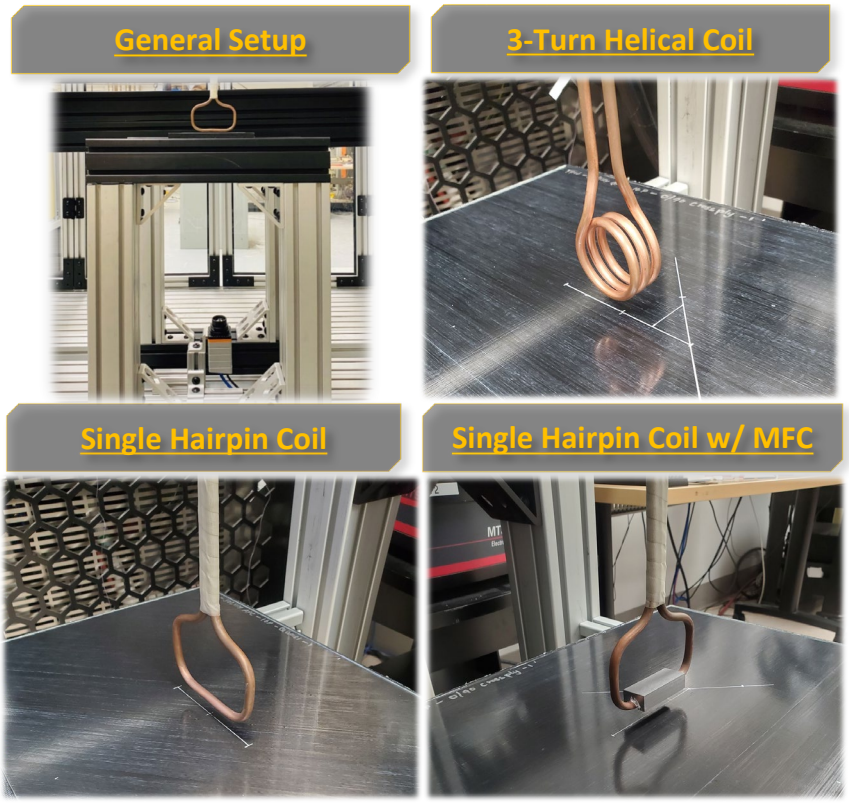

Figure 2. Experimental heating setup and induction coil geometries.

3. ANALYSIS

To simulate the heating and cooling of the weld, Altair Flux, a finite element analysis (FEA) software with coupled electromagnetic and thermal physics, was used. Using this simulation, the effect of material properties, input power of the system, coil design geometry, and magnetic flux controller (MFC) on the temperature evolution on the laminate (surface and through thickness) can be studied. Additionally, dynamic transient induction heating can be simulated (i.e. allowing for a moving coil and/or substrate).

3.1 FEA Model

Figure 3 shows the main components of the FEA models for a 16-ply thermoplastic laminate using different induction coil designs as well as with and without magnetic flux controller.

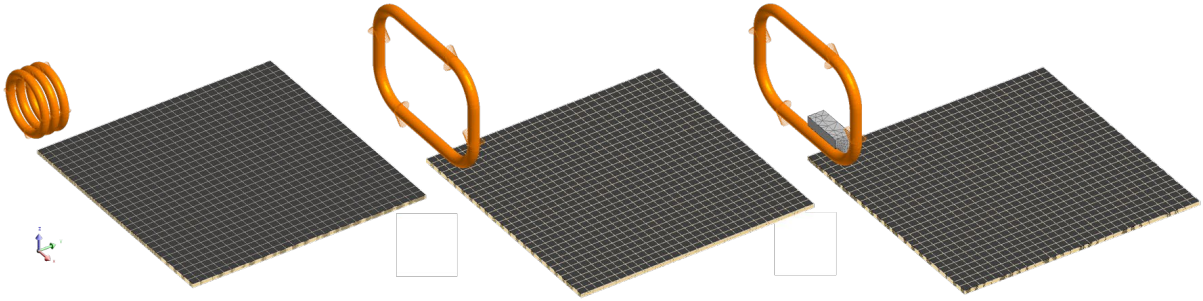

Figure 3. Altair Flux simulation model set-up for a) 3-turns helical coil, b) single hairpin coil, and c) MFC applied on single hairpin coil for a 16-ply laminate.

In Altair Flux, the non-mesh coil (macro feature) is a geometric entity that is superimposed on the computation domain and without a mesh as an alternative method for explicitly modelling the entire coil structure for simplicity and computational efficiency. The 3-turn helical coil was simplified into 3 circular coils with an outer diameter of 18.65 mm. The separation between the coils is 6.1 mm from its center and the radius of the circular tube cross-section is 2.4 mm. While the single hairpin coil was described as a rectangular coil with 19.05 mm fillet radius, outer perimeter of 95.25 mm, and 72 mm on the x and z directions, respectively. It has a circular cross-section as well with radius of 3.175 mm.

To examine the advantages of adding MFC during the induction heating process, a simple geometry of MFC is applied around the bottom part of the single hairpin coil. It is a rectangular prism with a cut-out slot to fit around the circular-cross section, with an overall dimension of 50.8 x 19.69 x 12.7 mm.

As mentioned in the introduction, one of the variables intended to study was the effects of stacking sequence on the temperature distribution of laminate on the surface and through the thickness. Thus, it is vital to setup a ply-by-ply model, which means it would have 16 separate volumes in a 16-ply laminate, assuming that all plies are perfectly in contact with each other. The surface area of each ply was modeled as 290 x 290 mm^2 with a 0.137 mm ply thickness. It is meshed with hexahedral elements and extruded along the laminate thickness. Table 1 summarized the geometrical parameters used in the FEA model.

Table 1. Summary of geometry inputs.

Property	**Value**
Laminate	
Surface area (mm^2)	290 x 290
Ply thickness (mm)	0.137
3-turns Helical Coil	
Loop radius (mm)	18.65
Pitch (mm)	6.1
Cross-section, tube diameter (mm)	4.8
Wall thickness (mm)	0.8125
Single Hairpin Coil	
Perimeter (mm)	95.25 x 72
Fillet radius	19.05
Cross-section, tube diameter (mm)	6.35
Wall thickness (mm)	0.794
Magnetic Flux Controller (MFC)	
Length, x (mm)	50.8
Width, y (mm)	12.7
Height, z (mm)	19.69

Assuming symmetry, a quarter-model was employed for the laminate and MFC (Figure 4) for computational efficiency. The entire model is surrounded by a 300 x 300 x 300 mm^3 infinite box while the volume region around the induction coil was finely meshed as structured elements with low relaxation coefficient (0.25) to account for the sharp thermal gradient in these zones. For the coil configurations selected, electromagnetic symmetry can be defined as follows: normal magnetic fields (MF) and tangent electric fields (EF) about the ZX plane (meaning we expect electrical current normal to this plane, but no magnetic fields normal to this plane), while this is opposite about the YZ plane with tangential magnetic field and normal electric field. Both symmetry planes were subjected to adiabatic heating conditions. Additionally, between the surface region of laminate and surrounding air, free convection heat transfer is applied with coefficient of 15 W/m^2K where 25 °C is set as the ambient temperature and initial temperature for the laminate is 30 °C.

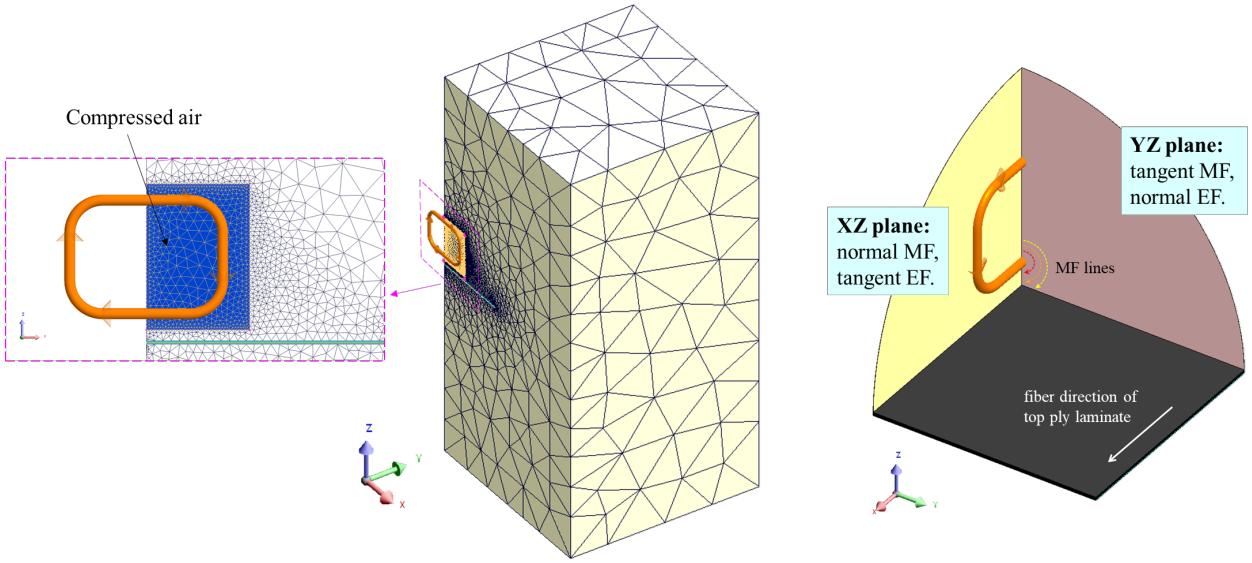

Figure 4. FEA model overview with local element meshing (left) and boundary conditions of symmetric planes (right).

3.2 Material Properties

To correctly simulate the inductive heating process, a large number of material properties need to be collected. According to Jackowski [2], the properties of composite materials are difficult to characterize due to their anisotropic nature; QI laminate are even more complex since each ply has its own properties in different directions resulting combined electrical interactions between plies causing highly complex (net) heating phenomenon. In this FEA model, material properties of the laminates were obtained from literature, whereas the properties of the induction coil and magnetic flux controller were imported from the material databases of Altair Flux. All data, together with their respective references, were summarized in Table 2.

In Table 2, the properties of laminates are listed in 0° laminate axes, meaning that these values are only associated with fiber direction along the x-axis in global domain. Thus, each layer is further oriented to its ply axes by defining an angle for each ply region to model the laminates as shown in Figure 5 based on the layup sequence.

Table 2. Summary of the material property inputs.

Property	**Laminate**		**Induction Coil**	**MFC**
Name	Solvay (Cytec APC PEKK-FC)		Copper	Fluxtrol50
Density (kg/m^3)	[1]1599		8960	-
Relative Permeability, μ_r	1		1	[6]59.64
Relative Permittivity, ε_r	[2]3.7		1	20
Electrical Resistivity, ρ (Ωm)	ρ_0	[3]4.37 x 10^{-5}	[4]3.66 x 10^{-6}	-
	ρ_{90}	[3]2.97 x 10^{-1}		
	ρ_z	[3]1.54 x 10^{0}		
Thermal Conductivity, λ (W/m°C)	λ_0	[1]4.06	[5]394	[5]9.7
	$\lambda_{90=z}$	[1]0.49		
Specific Heat Capacity, C_p (J/kg°C)	[1]25.22		[5]393	[5]482

[1]*Value at room temperature for a generic UD C/PEKK ply is shown, however from ref*erence [9] *curves defining the property with respect to temperature have been implemented.*

[2,3]*Value taken from the measurements and data collected in reference* [8,9].

[4]*Initial value at 0 °C is shown as taken from database of Altair Flux, however it is defining as linear function of T in the simulation.*

[5]*Isotropic, constant value from database of Altair Flux.*

[6]*Initial value is shown, however from Altair Flux database is defining as isotropic analytic saturation + knee adjustment (arctg, 3 coef.).*

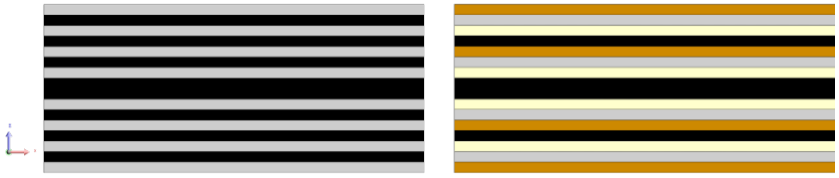

Figure 5. Through thickness view of the laminates (partial), each color indicates a fiber direction (left image is the CP laminate and right image is QI laminate).

3.3 FEA Solver Setup

The application was described as Steady State AC Magnetic coupled with Transient Thermal 3D. Two solvers were coupled; the Electromagnetic (EM) solver allows the power dissipated by Joule heating in the simulation model to be computed and then introduced as a heat source for the thermal solver. Simultaneously, the evolution of temperature in the model solved by thermal solver is applied to the EM solver for evaluating material properties. This is necessary since the effects of temperature-dependent properties is significant.

In this work, frequency (f) is held constant at 275 kHz. Figure 6 schematically illustrates the circuit system of the 3-turn helical coil. As previously mentioned in section 3.1, 3 circular non-meshed coils were used as the simplified version of the helical coil. Therefore, the stranded coil conductors in the circuit need to be connected in series to denote the coil as one unit. Single hairpin coil will not have any issue as it would only have a stranded coil conductor in the circuit.

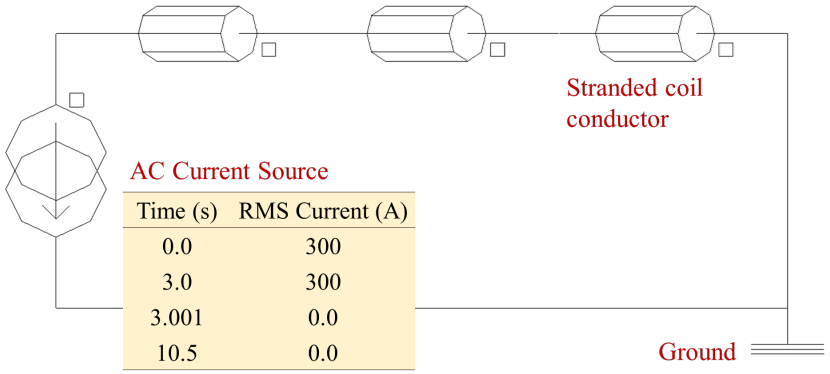

Figure 6. Circuit Context defined in Altair Flux for 300A heating case.

The total time of simulation is set to 10 seconds, allowing 3 seconds for the heating process and 7 seconds to simulate the cooling behavior of the laminate. Multiple levels of current input were applied to the model with a step value of 100A from 100A to 400A for all models without MFC applied and a step value of 50A from 100A to 250A for models with MFC applied. The distance from the bottom edge of the coil to the top surface of the laminate was set to 12.4 mm and this was held consistent throughout all the models included in this investigation.

4. RESULTS

4.1 Cross-ply Laminate, $[0/90]_{4s}$ Validation

Temperature history data of the laminates are recorded and plotted in Figure 7 for induction heating and cooling of each run with different coils and current inputs. The measurement point is directly below the coil centered on the non-coil side (NCS) of the laminate surface. The plot shows that the simulation prediction agrees well with the experimental results; the highest temperature deviation of ~10°C was noted between experimental and simulation results at max temperature.

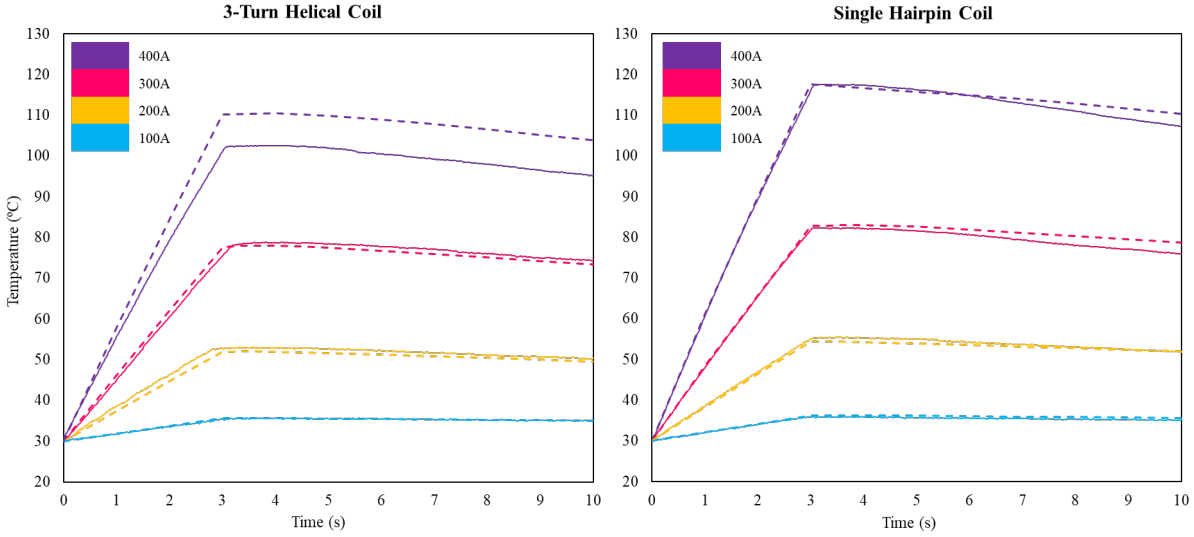

Figure 7. Temperature history data (solid line represents the real-time experiment data, while the dashed line represents the Altair Flux predictions).

The heating behavior on the NCS laminate surface at t=3s made by different coils and current inputs are shown in Figure 8. The highest temperature observed was right under the coil center, and the active heated region observed to be a projection of the coil (an elliptical shape). Quantitatively and qualitatively, the simulated temperature distribution agrees well with the experimentally obtained distributions.

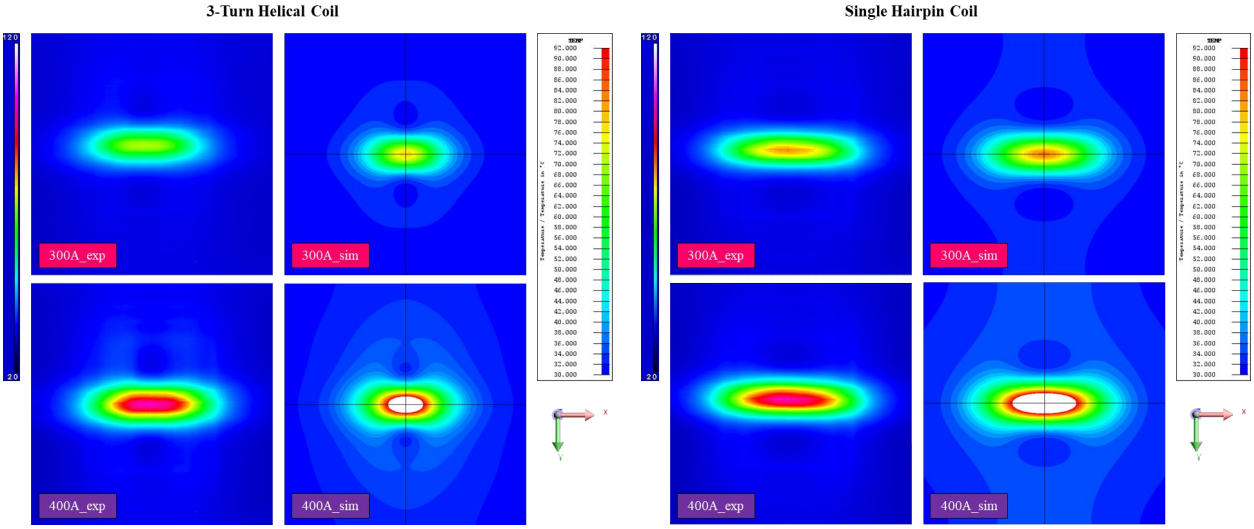

Figure 8. NCS surface thermal profile on laminate at t = 3s obtained from experiments (exp) and the FEA simulations (sim).

4.2 Magnetic flux controller

Figure 9 summarizes the laminate heating behavior with a MFC applied to the single hairpin coil. The MFC demonstrates improved heating efficiency, reaching the same max temperature and heat distribution as the 400A case shown in Figures 7 and 8, respectively, with only 200A current input. Furthermore, the high-heat region tends to be more concentrated and controllable which help reducing the edge effects during the welding process. Figure 10 shows the alteration of the magnetic field by MFC.

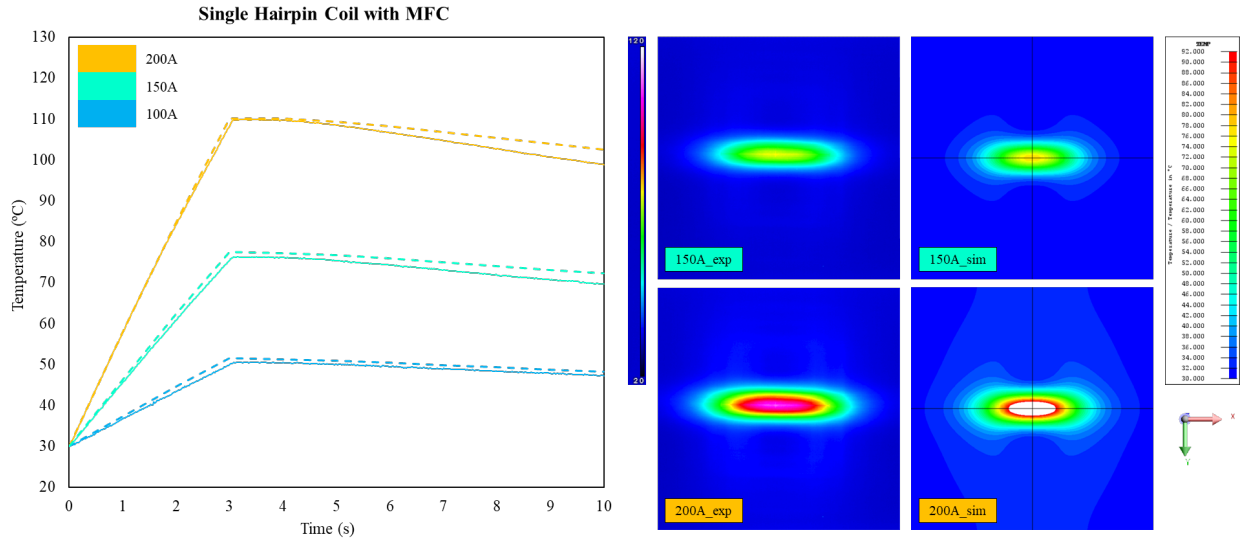

Figure 9. Temperature history and spatial temperature field comparisons for the single hairpin coil with MFC from experiments and simulations.

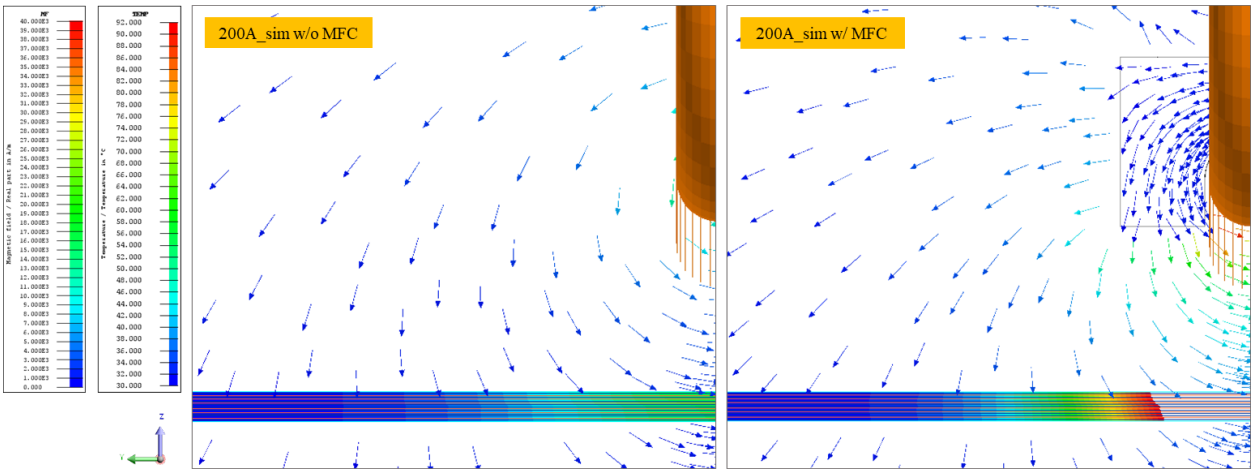

Figure 10. Magnetic field visualization of with (right) or without (left) MFC during induction heating process from FEA simulation.

4.3 Quasi-isotropic Laminate, $[45/0/-45/90]_{2s}$ Validation

The same study has been performed with a QI laminate. As can be seen in Figure 11, unlike for the case of CP laminates, the QI simulations do not match the experiments, although the general qualitative shape of the temperature field is similar (Figure 12). One potential reason for this discrepancy is the symmetric boundary conditions. From a homogenized global perspective, it is appropriate to assume normal or tangential electric current flow. However the presence of ±45° plies means that locally this assumption will not be valid in those plies.

Another simulation challenge is the way adjacent plies overlap and interact with each other. Although this model has neglected alternate heating mechanisms (contact resistance and dielectric hysteresis), the effect of contact resistance can be built-in to an effective resistivity for a given laminate. These simulation results seem to show that the resistivity we have modeled is accurate for a CP laminate, but not for a QI laminate.

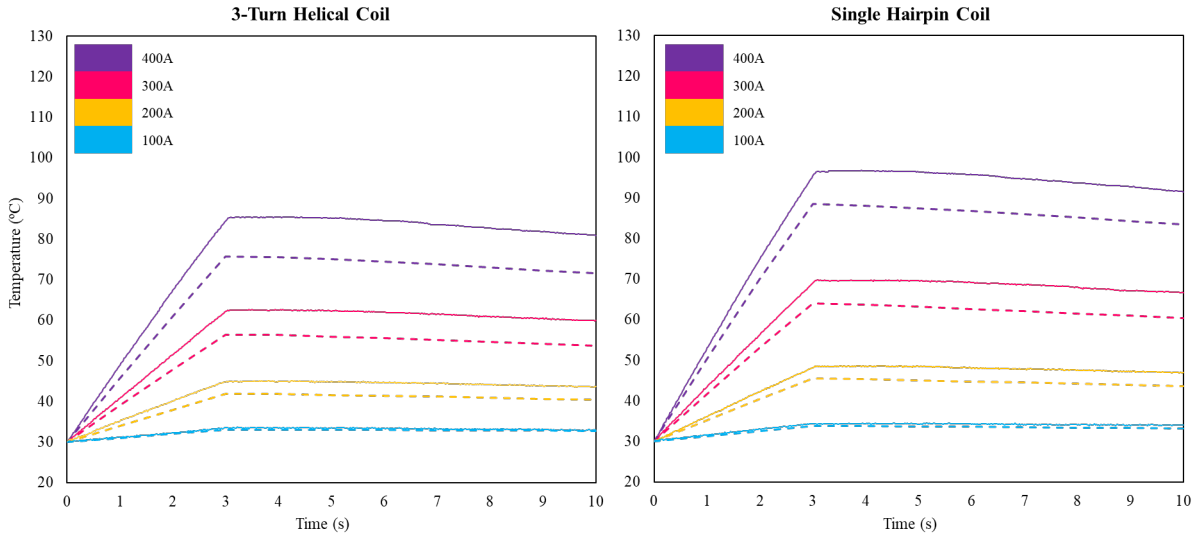

Figure 11. Temperature history for quasi-isotropic laminate (solid line represents the experimental data, while dashed line represents the Altair Flux predictions).

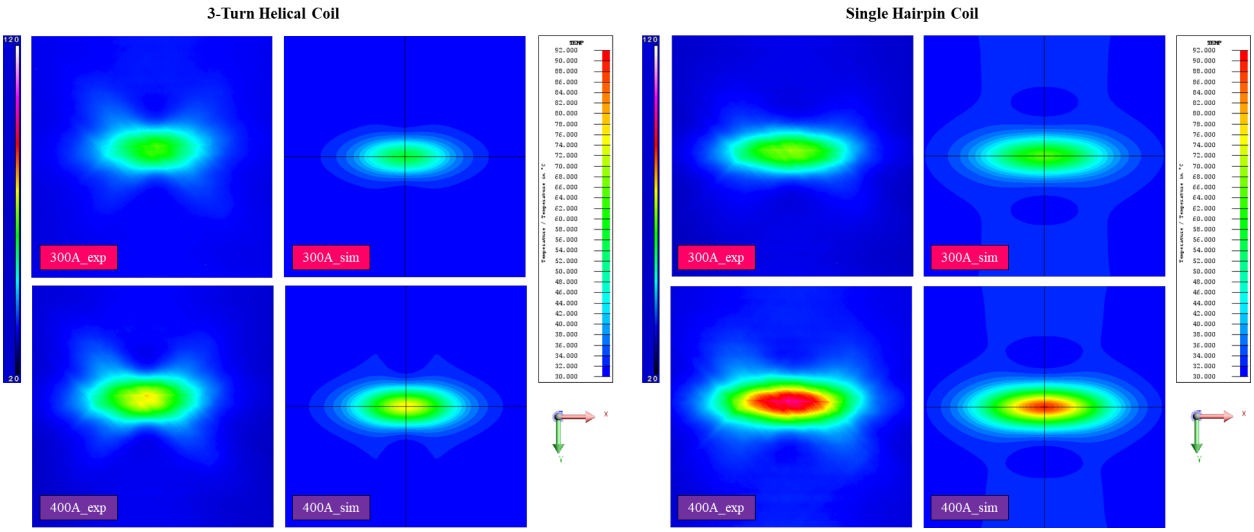

Figure 12. Spatial temperature field determined from heating trials and simulations for QI laminate.

4.4 Heating Rate Comparison

The inducting heating rate of all runs in this work has been summarized in Table 3. Overall, the CP laminate exhibits the highest rate of heating compared to the QI laminate both in experiments and simulations. This is because of the increased number of orthogonal ply intersections which promotes the formation of eddy currents. Regarding the accuracy of simulation predictions, the heating rate of CP and QI laminates has an average difference of 3% and 13%, respectively. For coil configurations, in all cases, the single hairpin coil offers better efficiency compared to the 3-turn helical coil for a given current input. Furthermore, the integration of MFC increased the heating rate by 230%.

Table 3. Comparison of induction heating rates, (°C/s).

	CP Laminates						**QI Laminates**			
	3-Turn Helical		Single Hairpin		Single Hairpin (MFC)		3-Turn Helical		Single Hairpin	
Current (A)	exp	sim	exp	sim	exp	sim	exp	sim	exp	sim
100	1.8	1.9	2.0	2.1	6.7	7.1	1.1	1.0	1.4	1.3
200	7.9	7.3	8.3	8.1	26.2	26.4	4.9	4.0	6.1	5.2
300	15.4	15.8	17.4	17.5	-	-	10.7	8.8	13.0	11.3
400	23.6	27.0	28.8	29.9	-	-	18.3	15.3	21.9	19.5

5. CONCLUSIONS

This work has demonstrated the potential of using Altair Flux, electromagnetic-thermal coupled finite element software to support the induction welding process development and optimization for thermoplastic composites. In this study, CP and QI CF/PEKK laminates were heated and validated with simulation model predictions. The effect of stacking sequences, relation of coil

geometry to temperature distribution, and the advantage of applying magnetic flux controller in the induction heating process was simulated and validated with experimental results. The simulation predicted the experimental heating rate within an average of 3 % for CP laminates and 13 % for QI laminates. A large increase in heating rate was noticed with the addition of a MFC on the induction coil. Techniques and methods of modeling the induction heating process were provided, such as the simplification of coil geometry and implementation of symmetry, which is useful for simulating the welding process for more complex geometries in the future.

6. ACKNOWLEDGEMENTS

This work is performed as a part of the Air Force Research Laboratory sponsored research project titled Modeling for Affordable Sustainable Composites (FA8650-19-C-5212). Authors would like to acknowledge the support from Dr. David Mollenhauer and the research team at NIAR/WSU. The authors gratefully acknowledge the technical support from Altair Flux. Facts and opinions are solely the personal statements of the authors and do not necessarily represent the views of the sponsoring agency.

7. REFERENCES

1. Van Ingen, J. W., Buitenhuis, A., Van Wijngaarden, M., *Development of the Gulfstream G650 induction welded thermoplastic elevators and rudder*, SAMPE 2010 Seattle, WA 2010, Society for the Advancement of Material Process and Engineering.
2. J.K. Jackowski, Robert C. Goldstein and V.S. Nemkov, Induction Process and Coil Design for Welding of Carbon Fiber Reinforced Thermoplastics, January 1, 14.
3. H.J. Kim, S. Yarlagadda, N.B. Shevchenko, B.K. Fink and J.W. Gillespie, *Development of a Numerical Model to Predict In-Plane Heat Generation Patterns During Induction Processing of Carbon Fiber-Reinforced Prepreg Stacks*, Journal of Composite Materials 37 (2003), pp. 1461–1483. DOI: 10.1177/0021998303034460.
4. P. Mitschang, R. Rudolf and M. Neitzel, *Continuous Induction Welding Process, Modelling and Realisation*, Journal of Thermoplastic Composite Materials 15 (2002), pp. 127–153. DOI: 10.1177/0892705702015002451.
5. B.K. Fink, R.L. McCullough and J.W. Gillespie, *A model to predict the planar electrical potential distribution in cross-ply carbon-fiber composites subjected to alternating magnetic fields*, Composites Science and Technology 49 (1993), pp. 71–80. DOI: 10.1016/0266-3538(93)90023-A.
6. W. Lin, A.K. Miller and O. Buneman, *Predictive capabilities of an induction heating model for complex-shape graphite fiber/polymer matrix composites*, 24 (1992), pp. T606–T620W. Lin, A.K. Miller and O. Buneman, *Predictive capabilities of an induction heating model for complex-shape graphite fiber/polymer matrix composites*, 24 (1992), pp. T606–T620.
7. S. Bensaid, D. Trichet and J. Fouladgar, *Electromagnetic and thermal behaviors of multilayer anisotropic composite materials*, IEEE Transactions on Magnetics 42 (2006), pp. 995–998. DOI: 10.1109/TMAG.2006.870926.

8. W.J.B. Grouve, F. Sacchetti, E.J. Vruggink and R. Akkerman, *Simulating the induction heating of cross-ply C/PEKK laminates – sensitivity and effect of material variability*, Advanced Composite Materials (2020), pp. 1–22. DOI: 10.1080/09243046.2020.1783078.
9. A. Yousefpour and M. Hojjati, *Welding Thermoplastics and Thermoplastic Composite Materials*, John Wiley & Sons, Chichester, United Kingdom, 2011.